

# Calculation of the cross section for the pion diffractive dissociation into two jets

V.L. Chernyak and A.G. Grozin

Budker Institute of Nuclear Physics,  
630090 Novosibirsk, Russia

## Abstract

Contribution of the gluon distribution in the nucleon to the cross section for the pion diffractive dissociation into two jets has been calculated recently. In addition, we present here calculation of contribution of the quark distributions to this process.

It is expected usually that the quark contributions are much smaller than the gluon one at high energies. We show that, under the conditions of the E791 experiment, the quark contributions are as significant as the gluon one, so that the total cross section exceeds several times those with only gluon contribution.

Nevertheless, the distribution of jets in longitudinal momentum fractions does not change significantly and remains qualitatively the same. We compare our results with the data from the E791 experiment.

**1.** The E791 experiment at Fermilab [1] has measured recently the cross section of the hard diffractive dissociation of the pion into two jets. In particular, the distribution of the total pion longitudinal momentum into fractions  $y_1$  and  $y_2 \equiv 1 - y_1$ , between jets has been measured. This distribution is potentially of great interest because its form depends on the pion wave function profile. So, its measurement can be used to obtain information about properties of the nonperturbative pion wave function  $\phi_\pi(x_1)$  which describes the distribution of quarks inside the pion in the longitudinal momentum fractions  $x_1$  and  $x_2 \equiv 1 - x_1$ .

This cross section has been calculated in the papers [2] and [3]<sup>1</sup>, in the approximation when only the contribution of the gluon distribution in the nucleon has been accounted for, while those of the quark distributions were neglected. The purpose of this paper is to account for these quark contributions. As will be shown below, the quark contributions are as significant as the gluon one and increase the amplitude by about a factor of two.

The paper is organized as follows. We explain our approach and consider some examples of diagrams in sect.2. Our main analytic results are presented in sect.3. The numerical calculations and comparison with data are given in sect.4.

**2.** We use the same approach as in [2] and a very similar notation. So, the presentation will be given in a short form and we refer to [2] for more detail.

The diagram in fig. 1 shows our notation and kinematics of the quark contributions to the amplitude. The function  $q_i(v, \xi)$  in fig. 1 denotes any of the quark distributions of the nucleon:  $i = (u, d, s, \bar{u}, \bar{d}, \bar{s})$ . The blob  $M$  represents the hard kernel of the process. It is proportional to the scattering amplitude

$$d(x_1 p_\pi) + \bar{u}(x_2 p_\pi) + q_i(q_1) \rightarrow d(p_1) + \bar{u}(p_2) + q_i(q_2) \quad (1)$$

of two initial pion quarks on the target quark. In the leading twist approximation, all six particles of this process can be considered as being on shell. Besides, the pion and target quarks can be considered as having zero transverse momenta, as account of primordial virtualities and transverse momenta results only in higher twist corrections to  $M$ .

---

<sup>1</sup>In comparison with their original calculation, the authors of [3] have found recently an additional missed contribution, so that their revised analytic results for the scattering amplitude agree now with those obtained in [2].

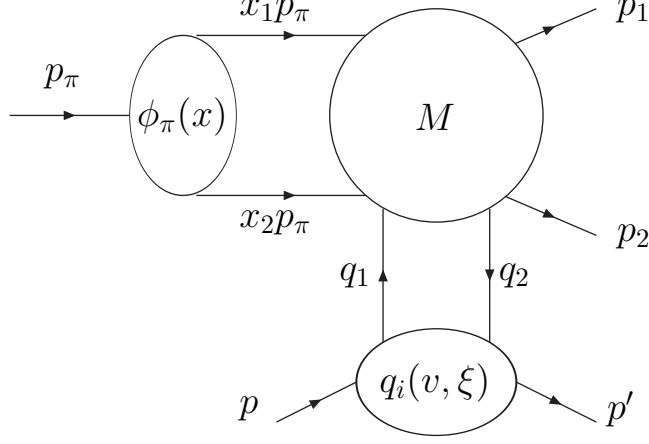


Figure 1: Kinematics and notations.

In the lowest order in  $\alpha_s$ ,  $M$  is given by a set of connected Born diagrams. Each diagram consists of three quark lines connected in all possible ways by exchanges of two hard gluons. There are eight such diagrams for each of six  $q_i$ . As an example, the representatives of three possible types of diagrams (scattering, annihilation and exchange) are shown in fig. 2 and fig. 3.

The quark and antiquark distributions in the nucleon are defined as ( $\hat{P} = \gamma_\mu P_\mu$ ):

$$\langle P' | \bar{q}(0)_\beta q(w)_\alpha | P \rangle = \frac{2\hat{P}_{\alpha\beta}}{4} \int_{-\xi}^1 dv \left\{ q(v, \xi) e^{-i(v+\xi)(\bar{P}w)} - \bar{q}(v, \xi) e^{i(v-\xi)(\bar{P}w)} \right\}, \quad (2)$$

where  $q = u, d, s$ , while the kinematical variables are:

$$\begin{aligned} q_1 &= (v + \xi)\bar{P}, & q_2 &= (v - \xi)\bar{P}, & \bar{P} &= (P + P')/2, \\ \Delta &= (q_1 - q_2) = 2\xi\bar{P}, & \xi &= \frac{\mathbf{k}_\perp^2}{2y_1 y_2 s}, & z_1 &= \frac{v + \xi}{2\xi}, & z_2 &= \frac{v - \xi}{2\xi}, \\ z_1 - z_2 &= 1, & 2(p_\pi \Delta) &= M^2 = \frac{\mathbf{k}_\perp^2}{y_1 y_2}, & & & & (3) \\ p_1 &= y_1 p_\pi + y_2 \Delta + k_\perp + (q_\perp/2), & p_2 &= y_2 p_\pi + y_1 \Delta - k_\perp + (q_\perp/2), \end{aligned}$$

where  $q_\perp$  is the small final transverse momentum of the nucleon while  $k_\perp$  is large.

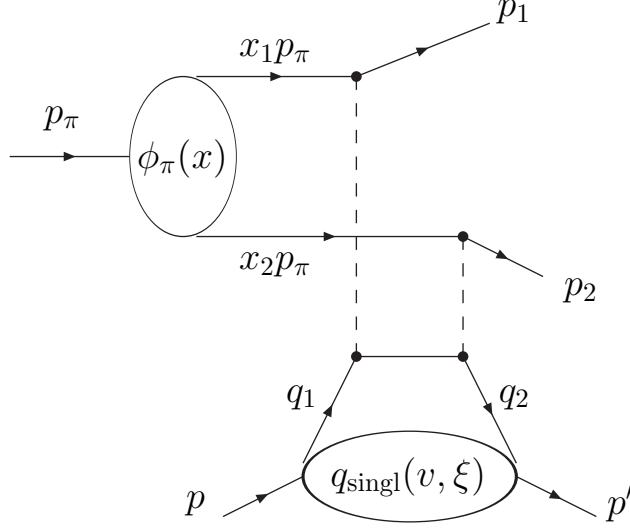


Figure 2: The scattering type diagram.

The structure of the amplitude is (symbolically):

$$T \sim \langle P' | \bar{q} \cdot q | P \rangle \otimes (\bar{\psi}_1 M \psi_2) \otimes \langle 0 | \bar{u} \cdot d | \pi^- \rangle, \quad (4)$$

where the first matrix element introduces the skewed quark and antiquark distributions of the nucleon,  $q_j(v, \xi)$  and  $\bar{q}_j(v, \xi)$ ,  $\bar{\psi}_1$  and  $\psi_2$  are the free spinors of final quarks,  $M$  is the hard kernel, i.e. the product of all vertices and hard propagators, the last matrix element introduces the pion wave function  $\phi_\pi(x)$ , and  $\otimes$  means the appropriate convolution.

As an example let us consider the diagram in fig. 2 as it gives the main contribution. Proceeding in the above described way (see also [2]), one obtains for the sum of the diagram in fig. 2 and the same diagram but with crossed gluon lines (the Feynman gauge is used for gluons):

$$T_0 = \frac{\rho_0}{y_1 y_2} \int_0^1 \frac{dx_1 \phi_\pi(x_1)}{x_1 x_2} \left\{ \int_{-\xi}^1 \frac{dv q_{\text{singl}}(v, \xi) [x_1 - y_1 - (v/\xi)]}{[v(x_1 - y_1) - \xi(x_1 y_2 + x_2 y_1)]} + (1 \leftrightarrow 2) \right\},$$

$$\rho_0 = \delta_{kl} \frac{(4\pi\alpha_s)^2 f_\pi}{27} (\bar{\psi}_1 \hat{\Delta} \gamma_5 \psi_2) \frac{(y_1 y_2)^2}{\mathbf{k}_\perp^4}; \quad (1 \leftrightarrow 2) \equiv \{x_1 \leftrightarrow x_2; y_1 \leftrightarrow y_2\}, \quad (5)$$

where  $k, l$  are the colour indices of final quarks. As it is expected that the imaginary part of the amplitude is the main one at high energies, we show

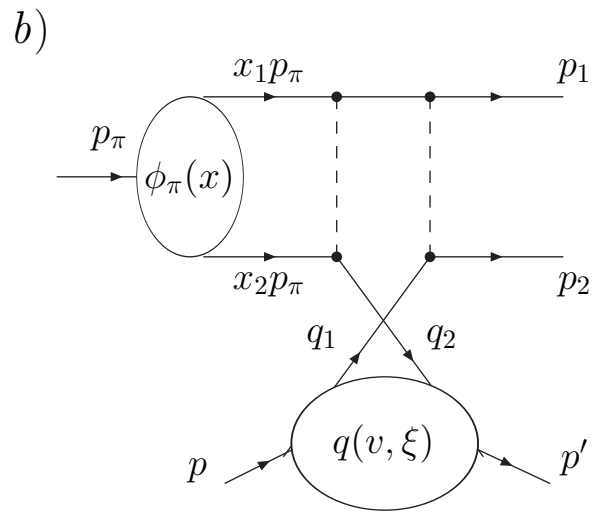
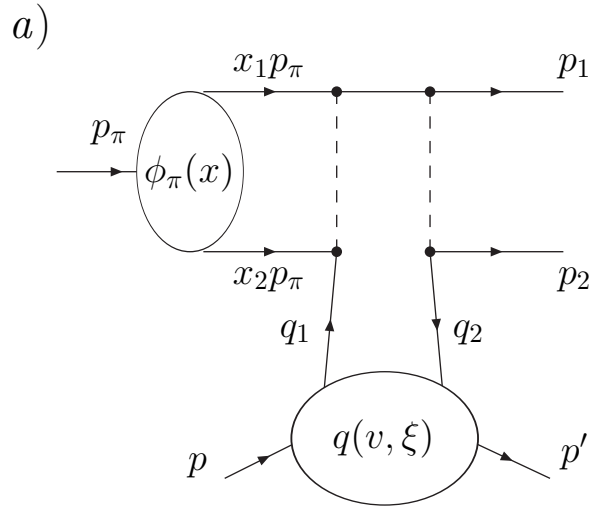


Figure 3: a) annihilation type diagram; b) exchange type diagram.

explicitly below only its value. From eq. (5) one obtains<sup>2</sup>:

$$\begin{aligned} \text{Im } T_0 &= \frac{\pi\rho_0}{y_1 y_2} \int_0^1 \frac{dx_1 \phi_\pi(x_1) (x_1 x_2 + y_1 y_2) q_{\text{singl}}(|\bar{v}|, \xi)}{x_1 x_2 (x_1 - y_1)^2} \Theta(|x_1 - y_1| > \delta), \\ q_{\text{singl}} &= \sum_{j=u,d,s} (q_j + \bar{q}_j), \quad \bar{v} = \xi \frac{x_1 y_2 + x_2 y_1}{x_1 - y_1}, \quad \delta = \frac{\mathbf{k}_\perp^2}{s}. \end{aligned} \quad (6)$$

As for all other diagrams, there are simple relations between contributions to the hard kernel  $M$  of different quark distributions for these diagrams:

$$\begin{aligned} M_{\bar{d}}(1, 2, v) &= -M_d(1, 2, -v); \quad M_{\bar{u}}(1, 2, v) = M_d(2, 1, v); \\ M_u(1, 2, v) &= -M_d(2, 1, -v). \end{aligned} \quad (7)$$

**3.** Summing up the contributions of all diagrams, one obtains for the total amplitude:

$$T_{\text{total}} = (T_{\text{gluon}} + T_0 + T_u + T_d + T_{\bar{u}} + T_{\bar{d}}), \quad (8)$$

where  $T_{\text{gluon}}$  is the contribution of the gluon distribution (see [2], eqs. (12–17)),  $T_0$  is given by eqs. (5–6), while the rest terms in eq. (8) are as follows:

$$\begin{aligned} \text{Im } T_j &= \frac{8\pi\rho_0}{3} \int_0^1 dx_1 \phi_\pi(x_1) \Sigma_j, \\ \Sigma_u &= \frac{q_u(\xi, \xi)}{x_1 y_2} + \frac{[x_1^2 x_2 - (x_1 - y_1)^3] q_u(|\bar{v}|, \xi) \Theta_+}{8|x_1 - y_1| x_1^2 x_2 y_1 y_2^2} + \frac{q_u(|\bar{v}|, \xi) \Theta_-}{8|x_1 - y_1| x_1 x_2^2}, \end{aligned} \quad (9)$$

where  $\Theta_+ = \Theta(y_1 + \delta < x_1 < 1)$ ,  $\Theta_- = \Theta(0 < x_1 < y_1 - \delta)$ ;

$$\begin{aligned} \Sigma_d &= \frac{(1 + y_1) q_d(\xi, \xi)}{x_1 y_1^2} \\ &+ \frac{(1 - 2x_1 x_2) y_2 q_d(\xi, \xi)}{8x_1 x_2^2 y_1^2} - \frac{[x_1 x_2^2 + (x_1 - y_1)^3] q_d(|\bar{v}|, \xi) \Theta_+}{8|x_1 - y_1| x_1 x_2^2 y_1^2 y_2} \\ &+ \frac{(1 - 2x_1 x_2) q_d(\xi, \xi)}{8x_1^2 x_2 y_1} - \frac{q_d(|\bar{v}|, \xi) \Theta_-}{8|x_1 - y_1| x_1^2 x_2}. \end{aligned} \quad (10)$$

$$\Sigma_{\bar{d}}(1, 2) = \Sigma_u(2, 1; q_u \rightarrow q_{\bar{d}}); \quad \Sigma_{\bar{u}}(1, 2) = \Sigma_d(2, 1; q_d \rightarrow q_{\bar{u}}). \quad (11)$$

---

<sup>2</sup>We introduce the terms  $i\epsilon$  into propagators through  $s + i\epsilon$ , i.e.  $\xi \rightarrow \xi - i\epsilon$  in all diagrams. Besides, it is implied that the quark distributions  $q_j(v, \xi)$  have simple zero at  $v = -\xi$ .

Let us note that while the separate terms in  $\int dx \phi_\pi(x) \Sigma_j$  are logarithmically divergent at  $x_{1,2} \rightarrow 0$ , it is not difficult to see that the divergences cancel in the sum, so that the integral is finite. This is an important point, as it shows that the whole approach is self-consistent, i.e. the hard kernel remains hard and the soft end point regions  $x_{1,2} \rightarrow 0$  give only power suppressed corrections.

Let us point out also that, unlike the gluon contribution, the quark contribution to the amplitude is not symmetric at  $y_1 \leftrightarrow y_2$ . However, this asymmetry is very small numerically in the main part of the phase space and becomes significant at the very edges  $y_{1,2} \rightarrow 0$  only, where the cross section is very small by itself.

The expressions (5–11) constitute the main result of this paper.

**4.** We present in this section the numerical estimates of the total cross section with account of both the gluon and quark contributions.

The quark distributions in the nucleon,  $q_j(v, \xi, t = 0, \mu)$  and  $\bar{q}_j(v, \xi, t = 0, \mu)$  at  $\mu \simeq k_\perp = 2 \text{ GeV}$ , are chosen in a simple form as (at  $v \geq \xi$  where we only need them):

$$\begin{aligned} q_u(v, \xi) &= 4 v^{-0.25} (1 - v)^3 + q_{\text{nonval}}(v, \xi), \\ q_d(v, \xi) &= 2 v^{-0.25} (1 - v)^3 + q_{\text{nonval}}(v, \xi), \\ \bar{q}_u = \bar{q}_d = q_s = \bar{q}_s &= q_{\text{nonval}}(v, \xi) = 0.13 v^{-1.2} (1 - v)^7. \end{aligned} \quad (12)$$

These forms agree reasonably well with the results of numerical calculations in [7] and [8]. The nuclear form factor is introduced as in [2], and we consider for comparison the same two model forms of the pion wave function:

$$\phi_\pi^{\text{asy}} = 6 x_1 x_2; \quad \phi_\pi^{\text{CZ}}(x, \mu \simeq 2 \text{ GeV}) = 15 x_1 x_2 [(x_1 - x_2)^2 + 0.2]. \quad (13)$$

Because the quark contributions have some asymmetry between the mirror points at  $y_1 < 0.5$  and  $y_1 > 0.5$ , while the experiment does not distinguish between the  $d$  and  $\bar{u}$  jets, we give below the answers for the cross sections symmetrized in  $y_1 \leftrightarrow y_2$  (i.e. the half sum of values at the mirror points).

To show the role of quark contributions we present in figs.4a and 4b the cross sections calculated with pure gluon distributions and the total cross sections (i.e. with account of both the gluon and quark distributions), for  $\phi_\pi^{\text{CZ}}$  and  $\phi_\pi^{\text{asy}}$  separately. It is seen that the cross section increases roughly 3 times with account of quark contributions. Let us illustrate in more detail how this happens for the case  $\phi_\pi^{\text{CZ}}$  at the middle point  $y_1 = y_2 = 0.5$ . For the

gluon distribution, the main contribution comes from the diagram in fig. 3 in [2] (the gluon analog of the diagram in fig. 2 in this paper). It contributes (36.2) to the amplitude in some units, while all other diagrams with the gluon distribution contribute (-19.3). So, the total gluon contribution becomes (16.9). The quark diagram in fig. 2 contributes (9.4), while all other quark diagrams contribute (2.9). So, the total quark contribution is (12.3), and it is quite comparable with the total gluon contribution. When moving from the middle point to the edges  $y_{1,2} \rightarrow 0$ , the role of quark contributions only increases. The picture for  $\phi_\pi^{\text{asy}}$  is very similar.

We show in fig. 5 the calculated total cross sections in comparison with the data from the E791 experiment [1]. Comparing these with the gluon contributions (see fig. 5 in [2]) one sees that the difference between  $\phi_\pi^{\text{CZ}}$  and  $\phi_\pi^{\text{asy}}$  becomes slightly more pronounced, but the main characteristic properties of the distribution of jets in  $y$  remained the same. I.e., the cross section is not much sensitive to the profile of the pion wave function  $\phi_\pi(x)$ . It seems that the present experimental accuracy is insufficient for obtaining stringent enough restrictions on the form of the pion wave function from these data.

Besides the experimental accuracy, it will be desirable, in addition, to improve the theoretical accuracy: to find one loop corrections to the hard kernels, to estimate higher twist corrections, to account for the real part of the amplitude, etc. Moreover, the main contributions from the diagram in fig. 3 in [2] and the diagram in fig. 2 here are sensitive to the precise form of the gluon and quark distributions in the nucleon, which are considered as known in our approach. So, the dependence of the  $y$ -distribution of jets on allowed variations of the forms of  $g(v, \xi)$  and  $q_i(v, \xi)$  has to be considered in more detail also.

Finally, let us give some typical numbers for the absolute values of the cross sections. For  $E_\pi = 500 \text{ GeV}$ ,  $k_\perp = 2 \text{ GeV}$  and  $\phi_\pi^{\text{CZ}}$ :  $d\sigma_{\text{Pt}}^{\text{CZ}}/(dk_\perp^2 dy) \simeq 7.5 \cdot 10^{-2} \text{ mbarn} \cdot \text{GeV}^{-2}$  at the middle point  $y_1 = y_2 = 0.5$ . The ratio  $d\sigma^{\text{asy}}/d\sigma^{\text{CZ}}$  is  $\simeq 1.23$  at  $y_1 = 0.5$  and  $\simeq 0.68$  at  $y_1 = 0.25$ .



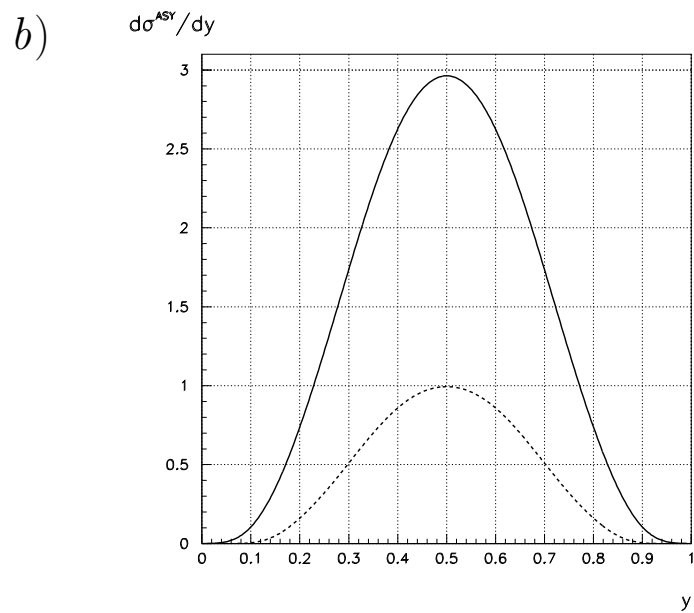
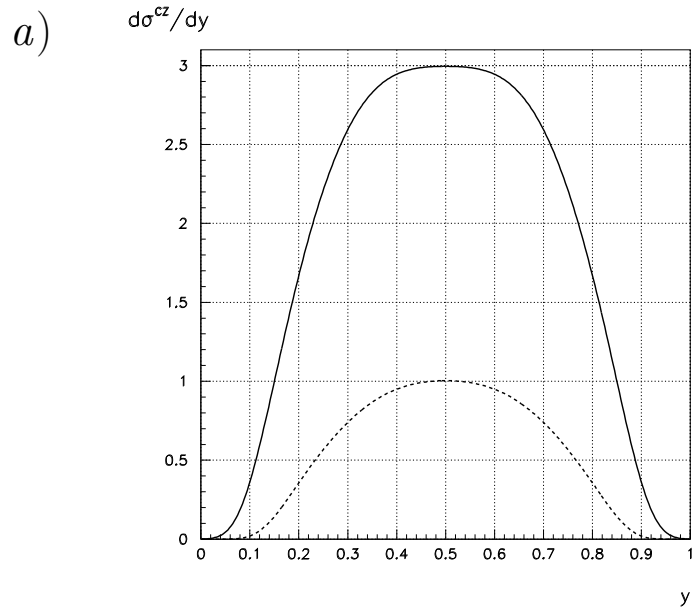


Figure 4: The relative values of the pure gluon (dashed line) and total (quark+gluon, solid line) cross sections for a)  $\phi_{\pi}^{CZ}(x)$  and b)  $\phi_{\pi}^{ASY}(x)$ .

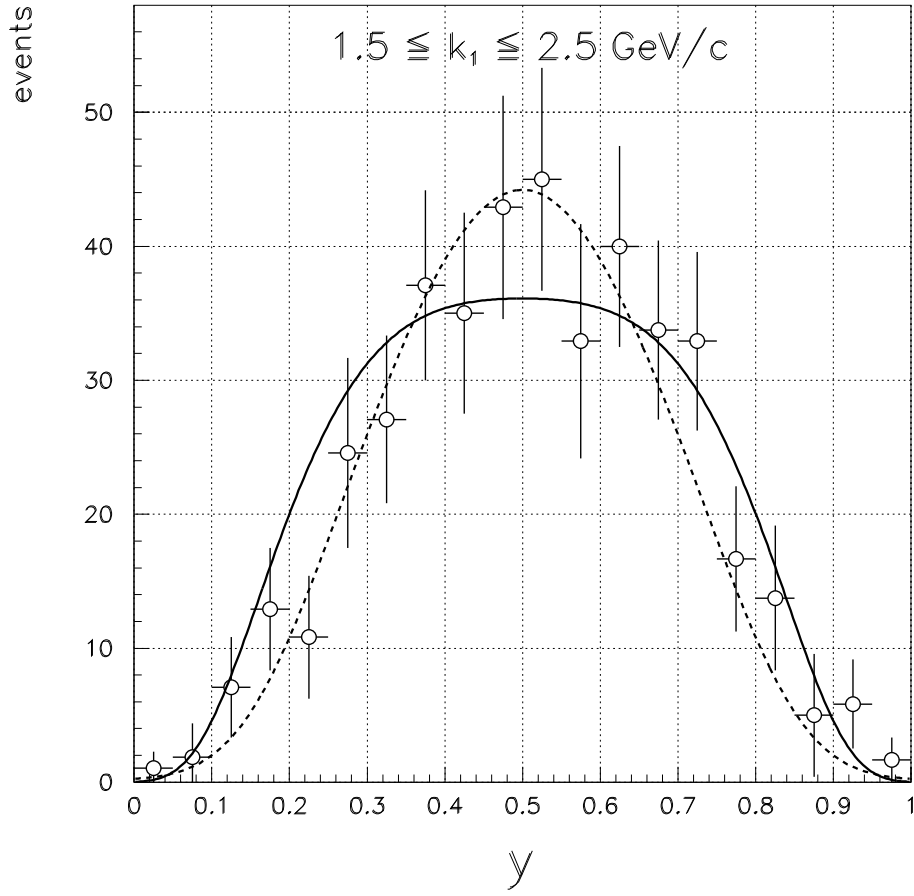


Figure 5: The  $y$ -distribution of jets for the total (quark+gluon) cross section, calculated for  $k_{\perp} = 2 \text{ GeV}$ ,  $E_{\pi} = 500 \text{ GeV}$  and with the pion wave functions:  $\phi_{\pi}^{CZ}(x, \mu \simeq 2 \text{ GeV})$  — solid line,  $\phi_{\pi}^{\text{asy}}(x)$  — dashed line. The overall normalization is arbitrary, but the relative normalization of two curves is as calculated. The data points are from the E791 experiment [1].

## References

- [1] E.M. Aitala et al. (E791 Collaboration), Phys. Rev. Lett. **86** (2001) 4768; hep-ex/**0010043**; D. Ashery, hep-ex/**9910024**; Invited Talk at X Intern. Light-Cone Meeting, Heidelberg, June 2000: hep-ex/**0008036**
- [2] V. Chernyak, hep-ph/**0103295**
- [3] V.M. Braun, D.Yu. Ivanov, A. Schafer and L. Szymanowski, Phys. Lett. **B509** (2001) 43; hep-ph/**0103275**
- [4] D. Muller, D. Robaschik, B. Geyer, F.-M. Dittes and J. Horejsi, Forts. Phys. **42** (1994) 101
- [5] A.V. Radyushkin, Phys. Lett. **B385** (1996) 333; Phys. Rev. **D56** (1997) 5524
- [6] X. Ji, Phys. Rev. Lett. **78** (1997) 610; J. Phys. **G24** (1998) 1181
- [7] M. Gluck, E. Reya and A. Vogt, Eur. Phys. J. **C5** (1998) 461
- [8] K.J. Golec-Biernat, A.D. Martin and M.G. Ryskin, Phys. Lett. **B456** (1999) 232; hep-ph/**9903327**